Available online at www.sciencedirect.com
ScienceDirect
Journal of Power Sources 174 (2007) 1258–1262
JOURNAL OF POWER SOURCES
www.elsevier.com/locate/jpowsour

Short communication

Conceptual design for 12 V "lead-free" accumulators for automobile and stationary applications

Kingo Ariyoshi, Tsutomu Ohzuku *

Department of Applied Chemistry, Graduate School of Engineering, Osaka City University (OCU), Sugimoto 3-3-138, Sumiyoshi, Osaka 558-8585, Japan

Available online 26 June 2007

Abstract

Conceptual design for 12 V lead-free accumulators is presented using basic research results on lithium insertion materials. Among possible materials, $Li[Li_{1/3}Ti_{5/3}]O_4$ is selected for a negative-electrode material, and $Li[Ni_{1/2}Mn_{3/2}]O_4$, $LiMn_2O_4$, $LiCo_{1/3}Ni_{1/3}Mn_{1/3}O_2$, and $LiFePO_4$ are specifically considered as positive-electrode materials. Combination of these materials with $Li[Li_{1/3}Ti_{5/3}]O_4$ gives a 2, 2.5 or 3 V lithium-ion battery. Series connection of such a lithium-ion battery makes 12 V lead-free accumulators possible. Characteristic features of the lead-free accumulators are discussed in terms of energy density for deep charge and discharge cycles, power density for short period of time, material economy, environmental friendliness, and safety compared with those of lead-acid batteries currently hold a position in automobile, large uninterruptible power supply, and off-grid solar home systems.

Keywords: Lead-free accumulator; Lithium-ion battery; Lithium titanium oxide; Lithium manganese oxide

1. Introduction

Lead-acid battery was invented in 1859 and developed largely during the past 145 years, which is still one of the most important secondary batteries for automobile and stationary applications. In lead-acid batteries, positive and negative electrodes consist of the chemical species of lead. The cell reaction widely accepted is $PbO_2 + Pb + 2H_2SO_4 \rightarrow 2PbSO_4 + 2H_2O$, which is called "double-sulfate" theory [1,2] meaning that discharge product of positive and negative electrodes is the same chemical species of $PbSO_4$. In this process, crystal structures of PbO_2 and Pb are completely destroyed to form $PbSO_4$ consuming H_2SO_4 in electrolyte, associated with expansion of electrodes. Therefore, improving dimensional instability of electrodes is a key issue to extend cycle life. Another point characteristic of lead-acid batteries is electrolyte, called flooded electrolyte. One hundred percent H_2SO_4 cannot be used in lead-acid batteries due to severe corrosion problems, so that diluted H_2SO_4 solution having specific gravity of about 1.2 corresponding to ca. 3.5 M H_2SO_4 is usually used in practical lead-acid batteries. This largely reduces specific capacities both in $Ah\,kg^{-1}$ and $Ah\,dm^{-3}$ and consequently energy densities in $Wh\,kg^{-1}$ and $Wh\,dm^{-3}$. As were briefly described above, lead-acid batteries are hard to say an appropriate system for high-energy density batteries in spite of the highest operating voltage of 2 V among aqueous batteries.

Lithium-ion battery was "born" in 1991 and rapidly advanced during the past 15 years. Characteristic features of lithium-ion batteries are: (1) lithium ions shuttle between positive and negative electrodes during charge and discharge (the amount of electrolyte can be minimized in contrast to lead-acid batteries), (2) the battery consists of two insertion materials in which lithium ions are inserted into/extracted from a solid matrix in a topotactic manner (change in electrode dimension is quite small compared to that in lead-acid battery), and (3) non-aqueous electrolyte is used (operating voltage is usually higher than 2 V). Lithium-ion batteries consisting of $LiCoO_2$ and graphite are quite popular as power sources for mobile phones and laptop computers. Lithium-ion batteries with capacity ranging from 550 mAh to 3 Ah are available in market, which are usually linked with the words of high-energy density, novel, precious, or advanced batteries. Therefore, it may be very hard for us to think of the possible application of lithium insertion materials to 12 V lead-free accumulators.

* Corresponding author.
E-mail address: ohzuku@a-chem.eng.osaka-cu.ac.jp (T. Ohzuku).

0378-7753/$ – see front matter © 2007 Elsevier B.V. All rights reserved.
doi:10.1016/j.jpowsour.2007.06.085

There are several lithium insertion materials reported during the past 15 years, such as $LiNiO_2$, $LiCo_xNi_{1-x}O_2$ ($0 \le x \le 1$), $LiAl_xNi_{1-x}O_2$ ($0 \le x \le 1/2$), $Li[Li_xMn_{2-x}]O_4$ ($0 \le x \le 1/3$), $LiNi_{1/2}Mn_{1/2}O_2$, $LiCo_{1/3}Ni_{1/3}Mn_{1/3}O_2$, $LiFePO_4$, $Li[Ni_{1/2}Mn_{3/2}]O_4$, $Li[Li_{1/3}Ti_{5/3}]O_4$, etc., as were reviewed by several authors [3–11]. However, application of new lithium insertion materials to lithium-ion batteries is usually difficult because current lithium-ion battery of $LiCoO_2$ and graphite is excellent in its performance. In this paper, we report conceptual design for lead-free accumulators based on lithium-ion battery concept with lithium insertion materials.

2. Selection of materials for 12 V lead-free accumulators

Single cell use of lead-acid battery is rare. Lead-acid batteries are usually used as 12 V batteries in which six cells are connected in series. Car electronics and power supply systems are usually based on 12 V power sources, i.e., 24, 36, and 48 V, due to long, long history of lead-acid batteries. Charge-end voltage of 12 V batteries is 13.8–14.8 V, corresponding to ca. 2.4 V of charge-end voltage for a single lead-acid battery. Capacities of 12 V batteries are usually 10–70 Ah, which are small in size for lead-acid batteries, but extremely large compared to those of current lithium-ion batteries. The batteries are normally left on float charge and always stored in a charged state. Twelve-volt automobile batteries are designed to provide extremely high current over a short period of time. Therefore, they are never discharged in full capacity. Deep-cycle lead-acid batteries are also designed for wheel chairs, forklift, and off-grid solar home systems. Limitation of 12 V lead-acid batteries is low energy density, especially gravimetric energy density, for stationary and wheeled applications. The batteries cannot be stored in a discharged state, and they show a limited number of cycles when the batteries are operated in full discharge cycles. Keeping in mind such situations for current 12 V batteries, we carefully selected lithium insertion materials for 12 V lead-free accumulators.

Fig. 1 shows the charge and discharge curves of lithium insertion materials. The structural and electrochemical properties are listed in Table 1. We select $Li[Li_{1/3}Ti_{5/3}]O_4$ (LTO) as a negative electrode for lead-free accumulators, because zero-strain insertion material of LTO is an ideal electrode material for long-life applications [12,13]. Operating voltage of LTO is ca. 1.55 V against lithium, so that dendritic growth of lithium on the negative electrode hardly takes place. In addition to the above merit in selecting LTO, thermal behavior of lithiated LTO is extremely milder than that of lithiated graphite [14]. This is necessary condition to make safe and long-life high-volume rechargeable batteries.

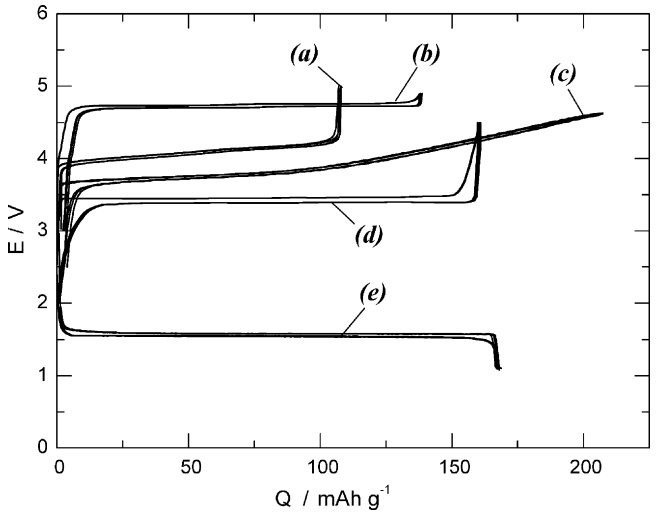

Fig. 1. Charge and discharge curves of lithium insertion materials selected for lead-free accumulators, (a) $LiMn_2O_4$-based material ($Li[Li_{0.1}Al_{0.1}Mn_{1.8}]O_4$: LAMO), (b) $Li[Ni_{1/2}Mn_{3/2}]O_4$, (c) $LiCo_{1/3}Ni_{1/3}Mn_{1/3}O_2$, (d) $LiFePO_4$ [20,21], and (e) $Li[Li_{1/3}Ti_{5/3}]O_4$ (LTO).

$LiMn_2O_4$-based materials having a spinel-framework structure are suitable for high-volume application [9], because λ-MnO_2 is more stable than delithiated $LiNiO_2$ or $LiCoO_2$ [15]. $LiMn_2O_4$-based material, $Li[Li_{0.1}Al_{0.1}Mn_{1.8}]O_4$ (LAMO), shows excellent cycleability with stable voltage profiles in spite of high-voltage operation in 3–5 V as shown in Fig. 1 [16]. $Li[Ni_{1/2}Mn_{3/2}]O_4$, which is also $LiMn_2O_4$-based material, shows the highest operating voltage of 4.7 V among the insertion materials reported so far with 135 mAh g^{-1} of rechargeable capacity [17]. $Li[Ni_{1/2}Mn_{3/2}]O_4$ shows topotactic two-phase reactions over an entire range, resulting in extremely flat operating voltage. Another possible electrode material selected is $LiCo_{1/3}Ni_{1/3}Mn_{1/3}O_2$, which is one of the manganese-based materials. $LiCo_{1/3}Ni_{1/3}Mn_{1/3}O_2$ shows such a unique character that change in lattice volume is extremely small, virtually no change for $0 < x < 2/3$ in $Li_{1-x}Co_{1/3}Ni_{1/3}Mn_{1/3}O_2$ corresponding to 0–175 mAh g^{-1}, so that long cycle life can be expected

Table 1
Structural and electrochemical parameters for lithium insertion materials selected for lead-free accumulators

	Lattice parameters (Å)	Density (g cm^{-3})	Theoretical capacity		Observed capacity[a], mAh g^{-1} (mAh cm^{-3})	Average voltage V vs. Li
			mAh g^{-1}	mAh cm^{-3}		
$LiMn_2O_4$ (LAMO)	$a = 8.24$	4.30	148	635	110[b] (455)	4.0
$LiCo_{1/3}Ni_{1/3}Mn_{1/3}O_2$	[c] $a = 2.86$, $c = 14.25$	4.75	278	1320	170 (805)	4.0
$Li[Ni_{1/2}Mn_{3/2}]O_4$	$a = 8.17$	4.46	147	655	140 (625)	4.7
$LiFePO_4$	$a = 10.33$, $b = 6.01$, $c = 4.69$	3.60	170	610	160 (575)	3.5
$Li[Li_{1/3}Ti_{5/3}]O_4$ (LTO)	$a = 8.36$	3.48	175	610	170 (590)	1.5

[a] Observed capacity means rechargeable capacity observed.
[b] Observed capacity of $LiMn_2O_4$ is calculated by using data for lithium aluminum manganese oxide (LAMO; $a = 8.21$ Å, $d = 4.16$ g cm^{-3}).
[c] Lattice parameters are given in hexagonal setting.

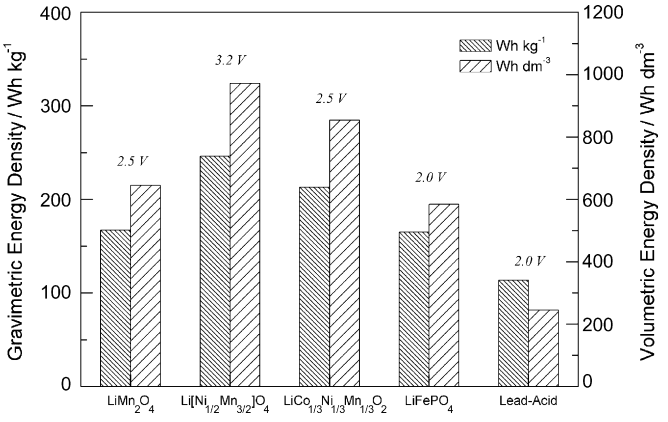

Fig. 2. Gravimetric and volumetric energy densities respectively in Wh kg^{-1} and Wh dm^{-3} calculated for possible lead-free accumulators based on LTO-negative electrode. In calculating the values, weight and volume calculated from structural data together with observed reversible voltage are used. The values for lead-acid batteries are also shown for comparison. For lead-acid batteries, Pb, PbO_2, and 5 M H_2SO_4 are considered in calculating energy density.

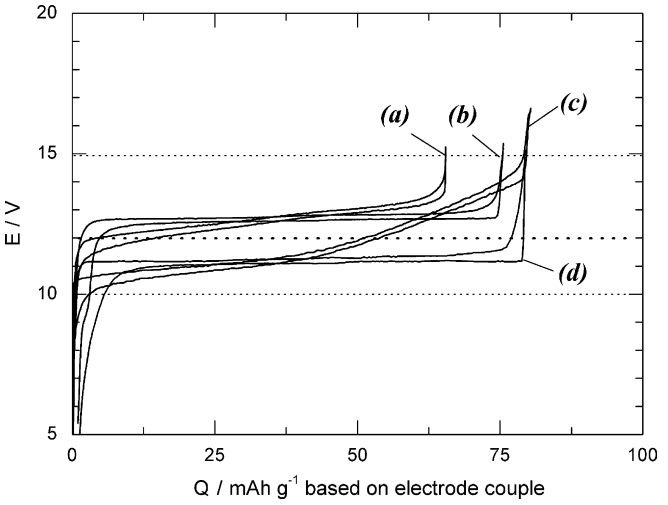

Fig. 3. Calculated voltage profiles for possible lead-free accumulators of LTO-negative electrode combined with (a) LAMO, (b) $Li[Ni_{1/2}Mn_{3/2}]O_4$, (c) $LiCo_{1/3}Ni_{1/3}Mn_{1/3}O_2$, and (d) $LiFePO_4$-positive electrode. These voltage profiles are calculated by using data in Fig. 1. To illustrate the curves, (a) 5, (b) 4, (c) 5, and (d) 6 cells are supposed to be connected in series.

[18]. This material shows better thermal stability than $LiNiO_2$ or $LiCoO_2$ [18,19]. Iron-based material of $LiFePO_4$ shows 3.5 V of flat operating voltage with 160 mAh g^{-1} of rechargeable capacity [20,21]. $LiFePO_4$ is one of the most attractive materials as far as safety issue is concerned, i.e., no exothermic reaction in temperature up to ca. 200 °C [22]. As seen in Fig. 1, operating voltage of these materials ranges from 3.5 to 4.7 V. Combination of these positive electrodes and LTO gives lead-free accumulators with different operating voltage, i.e., 2 V for $LiFePO_4$, 2.5 V for LAMO or $LiCo_{1/3}Ni_{1/3}Mn_{1/3}O_2$, and 3 V for $Li[Ni_{1/2}Mn_{3/2}]O_4$.

Energy density is a common measure to evaluate batteries. To estimate energy densities for possible lead-free accumulators, specific capacities and energy densities are calculated from observed values and listed in Table 2. In calculating specific capacities based on both active materials, called specific cell capacity hereafter in mAh g^{-1} and mAh cm^{-3}, we assume a balanced cell, i.e., $1/Q_{cell} = 1/Q_{PE} + 1/Q_{NE}$, where Q_{cell}, Q_{PE}, and Q_{NE} are specific cell capacities, rechargeable capacities for positive electrode, and negative electrode, respectively. Energy densities (W_{cell}) in Wh kg^{-1} and Wh dm^{-3} are calculated from specific cell capacity (Q_{cell}) and average voltage (E_{cell}), i.e., $W_{cell} = E_{cell} \times Q_{cell}$, for a balanced cell. The results are summarized in Fig. 2 and Table 2. Among them, LTO/$Li[Ni_{1/2}Mn_{3/2}]O_4$ battery shows the highest energy densities in both Wh kg^{-1} and Wh dm^{-3} mainly due to the highest operating voltage of 3.2 V. The value for LTO/LAMO seems to be small while operating voltage is the second highest value of 2.5 V. This is due to low observed capacity of 105 mAh g^{-1} for LAMO out of theoretical capacity of 148 mAh g^{-1} for $LiMn_2O_4$, suggesting that there is a space to improve the specific capacity.

It should be noted here that a grid of lead-based alloys to support positive and negative electrodes and a container to store flooded electrolyte of diluted H_2SO_4 are not counted when we calculate the energy density of lead-acid battery in Fig. 2. Such components are heavy and bulky for lead-acid batteries, so that real values are around 30 Wh kg^{-1} which are somewhere between one-tenth to one-fifth of the values in Fig. 2. In contrast to lead-acid batteries, light metal of aluminum or aluminum alloy can be used for both current feeder and cell case in fabricating lead-free accumulators based on lithium-ion battery concept. Therefore, values which can be attained are somewhere between one third to half of calculated values in Fig. 2.

To make 12 V lead-free accumulators, the batteries listed in Table 2 have to be connected in series. Fig. 3 shows calculated voltage profiles of 12 V lead-free accumulators by using basic data in Fig. 1, in which observed voltages as a function of specific capacity are used to illustrate charge and discharge

Table 2
Energy densities on lead-free accumulators of selected positive-electrode materials with LTO-negative electrode

Cell system	E_{cell}[a] (V)	Cell capacity (Q_{cell})[b]		Energy density (W_{cell})[c]		Number of cells for 12 V system
		mAh g^{-1}	mAh cm^{-3}	Wh kg^{-1}	Wh dm^{-3}	
LTO/$LiFePO_4$	2.0	82	290	165	585	6
LTO/LAMO	2.5	67	260	165	645	5
LTO/$LiCo_{1/3}Ni_{1/3}Mn_{1/3}O_2$	2.5	85	340	215	855	5
LTO/$Li[Ni_{1/2}Mn_{3/2}]O_4$	3.2	77	305	245	970	4

[a] E_{cell} is average voltage for a given cell system.
[b] Cell capacity for an electrode couple is calculated by using observed capacity for each electrode material, i.e., $1/Q_{cell} = 1/Q_{PE} + 1/Q_{NE}$.
[c] The energy density for an electrode couple are calculated from $W_{cell} = E_{cell} \times Q_{cell}$.

curves by assuming that positive- and negative-electrode capacities are well balanced under the given conditions. As seen in Fig. 3 and Table 2, 12 V lead-free accumulator can be made by connecting four cells in series for LTO/Li[$Ni_{1/2}Mn_{3/2}$]O_4, five cells for LTO/LAMO or LTO/$LiCo_{1/3}Ni_{1/3}Mn_{1/3}O_2$, and six cells for LTO/$LiFePO_4$. Among them, LTO/LAMO and LTO/Li[$Ni_{1/2}Mn_{3/2}$]O_4 systems are compatible with current 12 V lead-acid batteries. The LTO/$LiFePO_4$ cell is interesting for high-volume, long-life, and high-power applications, but operating voltage of 11 V is slightly low for some of 12 V applications. If $LiFePO_4$ is combined with graphite-negative electrode, flat operating voltage of ca. 3.3 V is expected [23], so that 12 V lead-free accumulator is possible when four cells are connected in series [24], which is comparable to that of Li[$Ni_{1/2}Mn_{3/2}$]O_4 and LTO. The LTO/$LiCo_{1/3}Ni_{1/3}Mn_{1/3}O_2$ cell also shows lower operating voltage than lead-acid batteries especially at the end of discharge. Sloping voltage profile for the LTO/$LiCo_{1/3}Ni_{1/3}Mn_{1/3}O_2$ cell may be suitable for HEV application. From these considerations, we select LAMO and Li[$Ni_{1/2}Mn_{3/2}$]O_4 with LTO for 12 V lead-free accumulators.

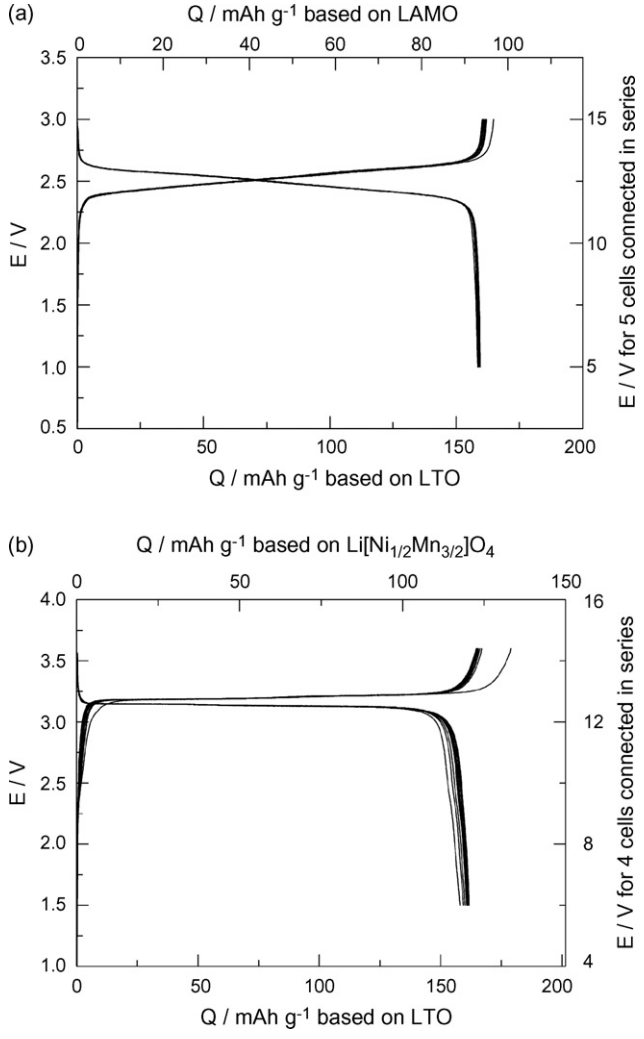

Fig. 4. Charge and discharge curves for the lead-free accumulator consisting of (a) LTO and LAMO or (b) LTO and Li[$Ni_{1/2}Mn_{3/2}$]O_4. Twelve-volt batteries can be made by connecting (a) 5 or (b) 4 cells in series.

3. Preliminary results on "lead-free" accumulators

Functions of 12 V lead-free accumulators may be high-power supply for short period of time for automobile applications and deep-discharge cycles for wheel-drive system and solar home systems. In order to examine whether or not such basic functions can be done for the lead-free accumulators, deep-discharge cycles at low current density and pulse discharge tests at high current density were carried out. Experimental conditions including material preparation, cell fabrication, and data acquisition, are the same as reported previously [25,26]. Fig. 4 shows the results on lead-free accumulators of LTO/LAMO and LTO/Li[$Ni_{1/2}Mn_{3/2}$]O_4. Charge and discharge curves of both cells for 10 cycles are shown in this figure. As seen in Fig. 4, voltage profiles are quite similar to calculated curves in Fig. 3. Steady voltage profiles are observed as were expected. Voltage drop to 1.5 V or less allows lead-free accumulators to stay in a discharged state. Zero-volt storage is possible, which cannot be done for lead-acid batteries, so that transportation of lead-free accumulators in a discharged state is easy compared to other batteries. Cycleability of lead-free accumulators of LTO/LAMO and LTO/Li[$Ni_{1/2}Mn_{3/2}$]O_4 are already reported [16,25]. Both show excellent cycleability more than 3600 cycles when we examined by accelerated cycle tests consisting of 6 min-constant voltage charge and 6 min-constant voltage discharge. Fig. 5 shows pulse discharge curves of LTO/LAMO and LTO/Li[$Ni_{1/2}Mn_{3/2}$]O_4 cells. Even when high current was applied to the cells (1 A g^{-1} based on LTO sample weight), discharge capacity over 150 mAh g^{-1} can be delivered for both systems. Polarization defined as a difference between voltages

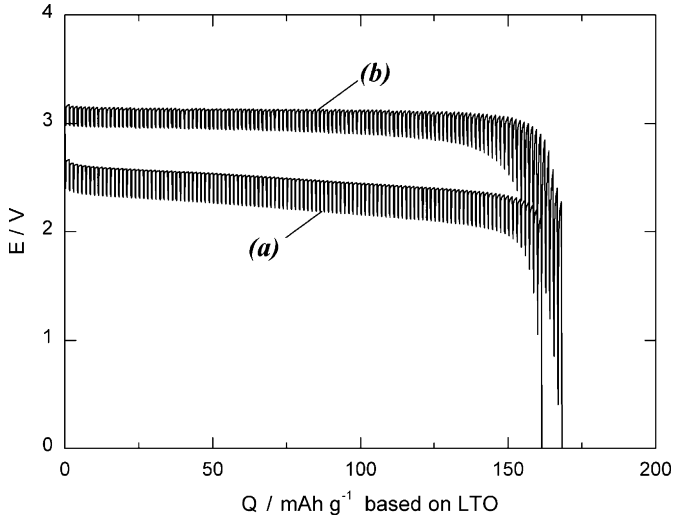

Fig. 5. Pulse discharge curves of (a) LTO/LAMO and (b) LTO/Li[$Ni_{1/2}Mn_{3/2}$]O_4 cells. A LTO/LAMO cell was operated at 12.2 mA cm^{-2} (1 A g^{-1} based on LTO weight or 0.57 A g^{-1} based on LAMO) for 5 s current on and 25 s off. LTO/Li[$Ni_{1/2}Mn_{3/2}$]O_4 cell was operated at 9.3 mA cm^{-2} (1 A g^{-1} based on LTO weight or 0.60 A g^{-1} based on Li[$Ni_{1/2}Mn_{3/2}$]O_4) for 5 s current on and 15 s off. Electrode consisted of (a) 88 wt% of LAMO or LTO, 6 wt% acetylene black (AB), and 6 wt% PVdF or (b) 80 wt% of Li[$Ni_{1/2}Mn_{3/2}$]O_4 or LTO, 10 wt% AB, and 10 wt% PVdF. Electrode mix weight is 73.2 mg for LAMO and 41.6 mg for LTO for (a), and 58.5 mg for Li[$Ni_{1/2}Mn_{3/2}$]O_4 and 34.9 mg for LTO for (b). Electrolyte used was 1 M $LiPF_6$ dissolved in EC/DMC (3/7 by volume). Two sheets of non-woven clothes were used as a separator.

at current on and off is almost constant over an entire range, indicating that the lead-free accumulators have enough capability to provide large burst of energy over a short period of time. In examining lead-free accumulators, we have applied non-woven cloth as a separator to reduce ohmic loss and to support electrolyte. If we select acetonitrile as a solvent and non-woven cloth as a separator, the lead-free accumulator in Fig. 5(a) shows more power than that examined in EC-based electrolyte [26], indicating that high-rate capability of lithium insertion materials is not limited by lithium-ion transport in a solid matrix, although pure acetonitrile is not applicable to lead-free accumulators because of low flashing point.

4. Concluding remarks

In this paper, we have reported conceptual design for 12 V lead-free accumulators for automobile and stationary applications in order to extend the applied field of lithium insertion materials. Through our trials on lead-free accumulators, we may contribute to renewable and clean energy technologies, such as solar and wind power systems with secondary batteries. This concept is based on lithium-ion battery, but shuttling ions between positive and negative electrodes are not limited to lithium ions. Other ions are quite possible if such insertion materials are available, so that we call 12 V lead-free accumulators. Basic researches on insertion materials are inevitably important to establish 12 V lead-free accumulators together with chemical and electrochemical methods to make series connection of battery easy and electrochemical methods to examine both capacity and power fade. Such basic researches are still under way in our laboratory.

Acknowledgements

The authors wish to thank Ms. Aiko Yamada, Mr. Takeshi Segawa, and Mr. Toru Kawai for their help on some of experimental works, and to Dr. Yoshinari Makimura, currently Toyota Central R&D Labs., Inc., for his help on preparing the manuscript. The present work was partially supported by a grant-in-aid from the Osaka City University (OCU) Science Foundation.

References

[1] G.W. Vinal, Storage Batteries, John Willy & Sons, Inc., NY, 1951.
[2] K. Kordesch, J.O'M. Bockris, in: B.E. Conway, E. Yeager, R.E. White (Eds.), Comprehensive Treatise of Electrochemistry, 3, Plenum Press, NY, 1981 (Chapter 3).
[3] J.R. Dahn, A.K. Sleigh, H. Shi, B.M. Way, W.J. Weydanz, J.N. Reimers, Q. Zhong, U. von Sacken, in: G. Pistoia (Ed.), Lithium Batteries: New Materials, Developments and Perspectives, Elsevier, Amsterdam, 1994, pp. 1–47.
[4] T. Ohzuku, A. Ueda, Solid State Ionics 69 (1994) 201–211.
[5] K. Sawai, Y. Iwakoshi, T. Ohzuku, Solid State Ionics 69 (1994) 273–283.
[6] M.M. Thackeray, Prog. Solid State Chem. 25 (1997) 1–71.
[7] M. Winter, J.O. Besenhard, M.E. Spahr, P. Novak, Adv. Mater. 10 (1998) 725–763.
[8] B. Ammundsen, J. Paulsen, Adv. Mater. 13 (2001) 943–956.
[9] G. Amatucci, J.-M. Tarascon, J. Electrochem. Soc. 149 (2002) K31–K46.
[10] M.S. Whittingham, Chem. Rev. 104 (2004) 4271–4301.
[11] T. Ohzuku, K. Ariyoshi, Y. Makimura, N. Yabuuchi, K. Sawai, Electrochemistry (Tokyo, Jpn.) 73 (2005) 2–11.
[12] T. Ohzuku, A. Ueda, N. Yamamoto, J. Electrochem. Soc. 142 (1995) 1431–1435.
[13] K. Ariyoshi, R. Yamato, T. Ohzuku, Electrochim. Acta 51 (2005) 1125–1129.
[14] J. Jiang, J. Chen, J.R. Dahn, J. Electrochem. Soc. 151 (2004) A2082–A2087.
[15] J.R. Dahn, E.W. Fuller, M. Obrovac, U. von Sacken, Solid State Ionics 69 (1994) 265–270.
[16] K. Ariyoshi, E. Iwata, M. Kuniyoshi, H. Wakabayashi, T. Ohzuku, Electrochem. Solid State Lett. 8 (2006) A557–A560.
[17] K. Ariyoshi, Y. Iwakoshi, N. Nakayama, T. Ohzuku, J. Electrochem. Soc. 151 (2004) A296–A303.
[18] N. Yabuuchi, T. Ohzuku, J. Power Sources 119–121 (2003) 171–174.
[19] I. Belharouak, Y.-K. Sun, J. Liu, K. Amine, J. Power Sources 123 (2003) 247–252.
[20] A.K. Padhi, K.S. Nanjundaswamy, J.B. Goodenough, J. Electrochem. Soc. 144 (1997) 1188–1194.
[21] A. Yamada, S.C. Chung, K. Hinokuma, J. Electrochem. Soc. 148 (2001) A224–A229.
[22] J. Jiang, J.R. Dahn, Electrochem. Comm. 6 (2004) 724–728.
[23] http://www.a123system.com/.
[24] http://www.valence.com/.
[25] K. Ariyoshi, S. Yamamoto, T. Ohzuku, J. Power Sources 119–121 (2003) 959–963.
[26] T. Ohzuku, K. Ariyoshi, Chem. Lett. 35 (2006) 848–849.